

# Histological, Immunohistochemical, and Biochemical Study of Experimentally Induced Fatty Liver in Adult Male Albino Rat and the Possible Protective Role of Pomegranate

Nadia F. Hassan, Gehan M. Soliman, Ebtsam F. Okasha, Amany M. Shalaby

Department of Histology, Faculty of Medicine, Tanta University, Tanta, Egypt

## Abstract

Nonalcoholic fatty liver disease is a major health problem and is considered the most common worldwide liver disease. Pomegranate has many biological activities and could modify the risk of hypercholesterolemia. The objective of the current research was to study the histological changes of experimentally induced fatty liver and possible protection by pomegranate. For this purpose, 50 adult male albino rats were divided into four groups, control group, pomegranate treated group that were given pomegranate juice for six weeks, fatty liver induced group that were fed on high fat diet for six weeks and protective group that were fed on high fat diet and received pomegranate juice for six weeks. Histological changes were detected in the fatty liver induced group in the form of disturbed hepatic architecture, dilatation and congestion of central veins, blood sinusoids and portal veins. Most of hepatocytes showed variable degrees of cytoplasmic vacuolation, mitochondrial structural changes, dilatation of endoplasmic reticulum in addition to nuclear structural changes like condensed chromatin, irregular shrunken nuclei and vacuolated nuclei. All these changes were associated with inflammatory cellular infiltrations, deposition of collagen fibers around the central vein, blood sinusoids, portal areas and in between the hepatocytes in addition to significant increase in number of hepatic stellate cells that was proved by electron microscope and confirmed by immunohistochemical study. Moreover, these structural changes were much less pronounced in animals treated with pomegranate either with or before receiving high fat diet. These findings suggested that pomegranate has a protective effect against experimentally induced fatty liver.

**Keywords:** Fatty liver, pomegranate, protective role

## INTRODUCTION

Liver is the largest metabolizing organ in the body which regulates homeostasis of different body systems. The main important functions of the liver include protein synthesis, storage, and metabolism of fats and carbohydrates, detoxification of drugs and other toxins, excretion of bilirubin and metabolism of hormones.<sup>[1]</sup>

Fatty liver refers to a large spectrum of diseases characterized by excessive fat accumulation in the liver which could be alcoholic or nonalcoholic fatty liver disease (NAFLD). The latter is clinically important because it affects about 25% of the population with widespread pathological changes in the liver that ranges from simple steatosis to steatohepatitis which can progress to cirrhosis, hepatocellular carcinoma and even liver failure with increased hepatic-related mortality.<sup>[2]</sup>

The increased hepatocellular lipids are correlated to central obesity, insulin resistance, dyslipidemia, and impaired glucose tolerance. The prevalence of NAFLD has reached epidemic proportions in recent years in parallel with the increasing prevalence of obesity. NAFLD is an early warning sign of future risk for Type 2 diabetes and cardiovascular disease.<sup>[3]</sup>

Herbs have been used by human being throughout the history from ancient primitive to modern time. Now herbs are one of the integral sources for the development of modern therapy.<sup>[4]</sup> *Punica granatum* or pomegranate is an edible fruit cultivated

**Address for correspondence:** Dr. Ebtsam F. Okasha,

Department of Histology, Faculty of Medicine, Tanta University, Tanta, Egypt.

E-mail: ebtsamokasha@gmail.com

This is an open access journal, and articles are distributed under the terms of the Creative Commons Attribution-NonCommercial-ShareAlike 4.0 License, which allows others to remix, tweak, and build upon the work non-commercially, as long as appropriate credit is given and the new creations are licensed under the identical terms.

**For reprints contact:** reprints@medknow.com

**How to cite this article:** Hassan NF, Soliman GM, Okasha EF, Shalaby AM. Histological, immunohistochemical, and biochemical study of experimentally induced fatty liver in adult male albino rat and the possible protective role of pomegranate. *J Microsc Ultrastruct* 2018;6:44-55.

### Access this article online

Quick Response Code:



Website:  
<http://www.jmau.org/>

DOI:  
10.4103/JMAU.JMAU\_5\_18

in Mediterranean countries, Asian countries, and some parts of the United States. It has been extensively used as a folk medicine by many cultures. It is a rich source of two types of polyphenolic compounds, anthocyanins, and hydrolyzable tannins which account for 92% of the antioxidant activity of the whole fruit. It has many biological activities such as anticarcinogenic, antibacterial, antidiarrheal, antifungal, anti-nephrolithiasis, antigastric ulceration, antiatherogenic, and chondroprotective effects. In addition, it could modify the risk of hypercholesterolemia and has photoprotective properties on the skin.<sup>[5]</sup>

This research was carried out to study the histological changes of experimentally induced fatty liver of adult male albino rat and to evaluate the effect of pomegranate in alleviating these changes.

## MATERIALS AND METHODS

### Animals

The present study was carried out on fifty adult male albino rats, weighing about 150–180 g each. They were housed in clean properly ventilated cages under similar conditions and had free access to rat standard laboratory diet and water throughout the experiment. The composition of the standard diet used in this study included 23.5% protein, 48.8% carbohydrate, 5% lipid, 12% water, 5% ash, 5% cellulose, and a 0.7% mixture of vitamins and minerals. The diet was designed at Tanta Company for oils and soap, Gharbia, Egypt. The animals were acclimatized to their environment at least 2 weeks before starting the experiment. All animals received human care in compliance with the guidelines of the Animal Care and Use Committee of National Research Center, Egypt. The experiment was approved by the Local Ethics Committee of Faculty of Medicine, Tanta University (Egypt).

### Preparation of pomegranate juice

The fresh pomegranate fruits, free of blemishes, or obvious defects were washed and stored at 4°C until use. The fruits were manually peeled, without separating the seeds. Pomegranate juice was obtained by squeezing using a commercial blender (Braun blender, Germany) and was filtered to remove the residue. The juice was used within 1 h after squeezing and filtration.<sup>[6]</sup>

### Preparation of high-fat diet

High-fat diet was prepared by adding 20% animal (lamb) fat +1% cholesterol to the standard diet.<sup>[7]</sup> Cholesterol was purchased from Sigma Company, Egypt which is in the form of white powder in plastic bottles each containing 100 g. The high-fat diet was prepared every 2 days, kept at 4°C until used and left at the room temperature 1 h before use.

### Experimental design

Following acclimatization, rats were randomly divided into four main groups:

- Group I (Control group): Included ten rats that were maintained on the standard diet for 6 weeks
- Group II (Pomegranate-treated group) included ten rats that were maintained on the standard diet and were given pomegranate juice orally by gastric tube at a dose of 20 ml/kg body weight daily for 6 weeks<sup>[8]</sup>
- Group III (Fatty liver induced group) included ten rats that were fed on high-fat diet for 6 weeks
- Group IV (Protective group) included twenty rats that were subdivided into two equal subgroups; ten rats each. Subgroup IV a: rats were fed on high-fat diet at the same composition and duration as in Group III concomitantly with pomegranate juice at the same dose and route as in Group II. Subgroup IV b: rats were maintained on the standard diet and given pomegranate juice for 6 weeks as in Group II then stopped and the rats were shifted from standard diet to high-fat diet as in Group III for another 6 weeks.

At the end of the experimental period, all rats were fasted overnight then anesthetized with ethyl ether.<sup>[9]</sup> Blood samples were immediately collected from the retro-orbital plexus with capillary tubes into clean dried centrifuge tubes. The tubes were then centrifuged at 3000 rpm for 15 min. Clear serum samples were carefully separated using Pasteur pipettes and frozen at –20°C until biochemical analysis.<sup>[10]</sup> Serum total cholesterol (TC), high-density lipoprotein cholesterol (HDL-c), and serum triglycerides (TGs) were measured with commercially available kits that were obtained from Biodiagnostic, Egypt.

Livers of the experimental animals were removed by careful dissection, washed with cold saline solution and dried between two filter papers then photographed for gross observation. The upper parts of the right lobes were taken and then divided into two parts, 0.5 cm<sup>3</sup> each. One part was fixed in 10% formal saline solution for preparation of paraffin blocks and other part was cut into very small pieces and fixed in 2.5% phosphate-buffered glutaraldehyde for electron microscopic study.

### Preparation of paraffin sections for light microscopic study

A piece of the right lobe of liver of each animal was taken and immediately fixed in 10% formal saline solution for 24 h. Dehydration was then carried out in ascending grades of alcohol followed by clearing with xylol. Impregnation was done in pure soft paraffin for 2 h at 50°C followed by embedding in hard paraffin. Sections of 3–5 microns in thickness from each block were cut by the microtome, then stained with hematoxylin and eosin stain to study the general histological structure<sup>[11]</sup> and Mallory's trichrome stain to demonstrate the collagen fibers.<sup>[12]</sup>

Some paraffin sections were stained using the avidin-biotin immunohistochemical technique for detection of glial fibrillary acidic protein (GFAP) within hepatic stellate cells. Universal kits for GFAP manufactured by Biogen Inc. (Cambridge, Massachusetts, USA) were obtained from Dako Company (Egypt). Sections were deparaffinized,

rehydrated, and rinsed in tap water, embedded in 3% hydrogen peroxide for 10 min then immersed in antigen retrieval solution. Nonspecific protein binding was blocked using blocking solution (phosphate-buffered solution [PBS] plus 10% normal goat serum). Sections were incubated for 2 h with the diluted primary antibody using PBS at different dilutions (1/500, 1/200, and 1/100) for biotinylated monoclonal mouse antibody for GFAP. Drops of streptavidin-peroxidase were added for 20 min then washed with PBS for 5 min. Diaminobenzidine was added to as chromogen and Mayer's hematoxylin was used as a counterstain. For negative control, the primary antibody was replaced by PBS.<sup>[13]</sup>

### Preparation of semithin and ultrathin sections for electron microscopic study

Liver specimens were divided by a sharp razor blade into small pieces of 1 mm<sup>3</sup> in size and were immediately fixed in 2.5% phosphate-buffered glutaraldehyde, after two to three rinses in the buffer they were post fixed in freshly prepared 1% phosphate buffer osmium tetroxide at 4°C for 1 h, then dehydrated in ascending grades of ethanol. After immersion in propylene oxide, the specimens were embedded in epoxy resin mixture. Semithin sections (1 mm thick) were stained with 1% toluidine blue and examined by light microscope for proper orientation while ultrathin sections (80–90 nm (were stained with uranyl acetate and lead citrate<sup>[14]</sup> to be examined by JEOL-JEM-100 transmission electron microscope) Tokyo, Japan) at the Electron Microscopic Unit, Faculty of Medicine, Tanta University.

### Morphometric study and statistical analysis

Collagen fibers' area% and GFAP +ve cell count in all groups were measured in image analysis system (Leica Qwin V3 program [Leica Microsystems] Switzerland. LTD) in Research Central Laboratory, Faculty of Medicine, Tanta, Egypt. All data (collagen fibers area%, GFAP +ve cell count, TC, TGs, and HDL-c) for all groups were expressed as mean ± standard deviation (SD) statistical analyses were carried out using SPSS software (SPSS Science, version 11.0.1, Chicago, Illinois, USA). The *post hoc* test was used to compare between groups. All data were expressed as means ± SD,  $P \leq 0.05$ , and 0.001 were considered significant and highly significant, respectively.

## RESULTS

No deaths were recorded in animals of all groups.

### Macroscopic results

Macroscopic examination of the livers from the control group and pomegranate received group showed normal red, smooth, and shiny appearance [Figure 1a and b]. On the contrary, livers obtained from fatty liver-induced group appeared enlarged, yellowish, and extensively infiltrated with yellow spots [Figure 1c], while livers obtained from protective group (subgroup IVa and subgroup IVb) showed red-brownish livers with smooth surfaces like that of the control group [Figure 1d and e].

## Light microscopic results

### Hematoxylin and eosin stain

#### Group I (control group)

Examination of sections obtained from livers of the control group showed normal histological structure. The liver was formed of classic hepatic lobules which were roughly hexagonal in shape with central veins forming their central axis. At their angles, there were portal areas containing connective tissue stroma and portal triads. The latter consisted of a terminal branch of the hepatic artery and a small branch of the portal vein as well as a bile ductule [Figure 2a and b]. Each classic hepatic lobule was formed of hepatocytes arranged in anatomizing cords, radiating from the center toward the periphery [Figure 2c]. The hepatocytes were polygonal in shape-containing rounded vesicular nuclei with dispersed chromatin and prominent nucleoli and others were binucleated. The cytoplasm of hepatocytes appeared acidophilic with scattered fine basophilic granules. Blood sinusoids were found as a network between the plates of hepatocytes converging toward the central vein. They were lined by two types of cells, the endothelial, and Kupffer cells. The endothelial cells appeared flattened forming discontinuous layer with darkly stained flat nuclei and Kupffer cells appeared scattered among the endothelial cells with large, rounded nuclei [Figure 2d].

#### Group II (pomegranate received group)

Examination of livers sections obtained from animals received pomegranate juice for 6 weeks were similar to the control group and showed the normal histological structure of the liver.

#### Group III (fatty liver-induced group)

Examination of livers sections obtained from this group revealed several histological changes in the form of disturbed hepatic architecture [Figure 3a], marked dilatation of central veins [Figure 3b] dilatation and congestion of portal veins [Figure 3c] and blood sinusoids [Figure 3d]. In addition to cellular infiltrations that can be seen around central veins [Figure 4a], around and in between the components of portal tract [Figure 4b and c] and even between the hepatocytes [Figure 4d] as well as proliferation of bile ductules [Figure 4c]. Most of the hepatocytes showed variable degrees of cytoplasmic vacuolations [Figures 3-5], some contained multiple small vacuoles [Figure 5a], some showed one large vacuole [Figure 5b], the others appeared ballooned with peripheral nuclei [Figure 5c]. In addition, some nuclear changes were observed like darkly stained (pyknotic) nuclei, fragmented nuclei (karyorrhexis), and lysed nuclei (karyolysis) [Figure 5c] hepatocytes with nuclear vacuolations (glycogenated nuclei) were also observed [Figure 5d]. Multiple small cells with ovoid nuclei (most probably hepatic stem cells [HSCs]) and arranged in rows were seen in between the hepatocytes [Figure 5b].

#### Group IV (protective group)

Examination of livers sections obtained from both subgroups (subgroup IV a and subgroup IV b) revealed results like each other in the form of mild congestion of the



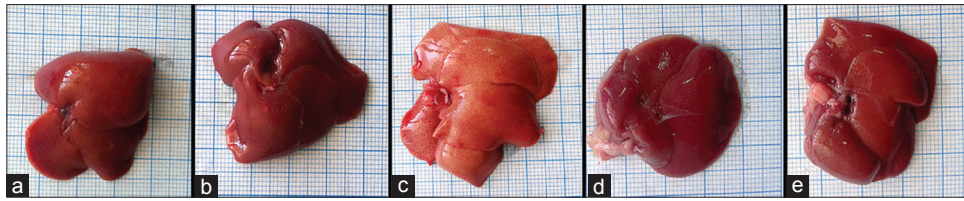


**Figure 1:** Gross macroscopic picture of the livers from the control group (a) and pomegranate-received group (b), both show reddish, smooth, and shiny liver surfaces. Apparent enlargement with yellowish spotty appearance is noticed in fatty liver-induced group (c). Livers from protective group either subgroup IV a (d) or subgroup IV b (e) are reddish brown with smooth surfaces

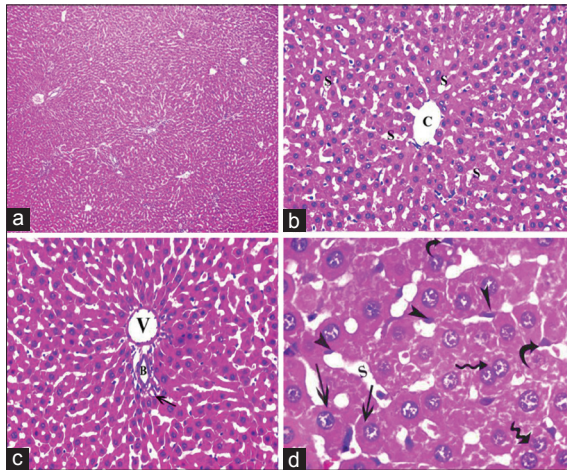


**Figure 2:** Photomicrographs of liver sections of control group showing: (a) Normal liver architecture. (b) A classic hepatic lobule-containing central vein (c) and radiating cords of hepatocytes with blood sinusoids (s) in between. (c) Portal tract at the periphery of a classic hepatic lobule revealing a portal venule (v), a hepatic arteriole (arrow) and a bile ductule (b). (d) Polyhedral hepatocytes with large, rounded vesicular nuclei (arrow) and prominent nucleoli, some binucleated cells are also present (waved arrow), blood sinusoids (s) are present in between the cords of hepatocytes and are lined by flattened endothelial cells (arrowhead) and Kupffer cells (curved arrow) (a: H and E,  $\times 100$ , b and c: H and E,  $\times 400$ , d: H and E,  $\times 1000$ )

central veins [Figure 6a], mild congestion, and dilatation of portal veins [Figure 6b] and blood sinusoids [Figure 6c and d] with few cellular infiltrations around the components of portal tracts [Figure 6b]. Most of the hepatocytes showed restoration of their cytoplasm, while few cells still showed some cytoplasmic vacuoles [Figure 6c and d].

#### *Mallory's trichrome stain*

Examination of Mallory's trichrome-stained sections of both control rats and rats received pomegranate only showed fine collagen fibers around central veins and portal tracts forming a common sheath [Figure 7a and b], while sections obtained from fatty liver-induced group revealed increased amount of collagen fibers around central veins and blood sinusoids [Figure 7c and d]. In addition, great amount of collagen fibers was detected around and in between portal tracts and in between the cords of hepatocytes [Figure 7e and f]. On the other hand, livers sections obtained from animals of both subgroups of the protective group revealed few collagen fibers around central veins and portal tracts [Figure 7g and h].

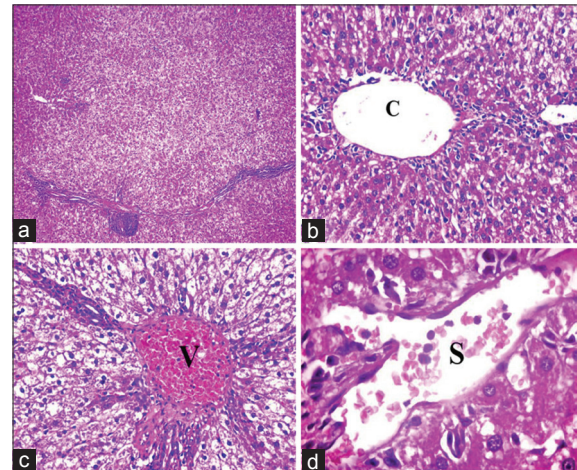


**Figure 3:** Photomicrographs of liver sections of Group III showing: (a) Disturbed liver architecture. (b) Apparently dilated central vein (C). (c) Apparently dilated and congested portal vein (V). (d) Apparently dilated and congested blood sinusoids (S). Notice vacuolation of most of hepatocytes (a: H and E,  $\times 100$ , b and c: H and E,  $\times 400$ , d: H and E,  $\times 1000$ )

#### *Glial fibrillary acidic protein immunohistochemical stain*

Examination of GFAP immunohistochemical-stained sections of both control group and pomegranate received group revealed GFAP positive cells in between the hepatocytes [Figure 8a]. Examination of GFAP immunohistochemical-stained sections obtained from fatty liver-induced group revealed apparent increase in number of GFAP-positive cells [Figure 8b], while in both subgroups of the protective group apparent decrease in number of GFAP positive cells were observed [Figure 8c].

#### **Electron microscopic results**

##### *Group I (control group)*

Examination of ultrathin sections of the livers obtained from control rats revealed the normal electron microscopic picture of the liver. The hepatocytes were polyhedral in shape containing large, rounded euchromatic nuclei with prominent nucleoli. The cytoplasm of the hepatocytes contains abundant cell organelles, mainly mitochondria which appeared rounded or oval, slightly variable in size and distributed throughout the cytoplasm in association with endoplasmic reticulum, secondary lysosomes, and glycogen that appeared as electron dense particles dispersed as single minute granules [Figure 9a and b]. HSCs with their characteristic nuclei and lipid droplets in their cytoplasm were observed in the spaces of Disse between



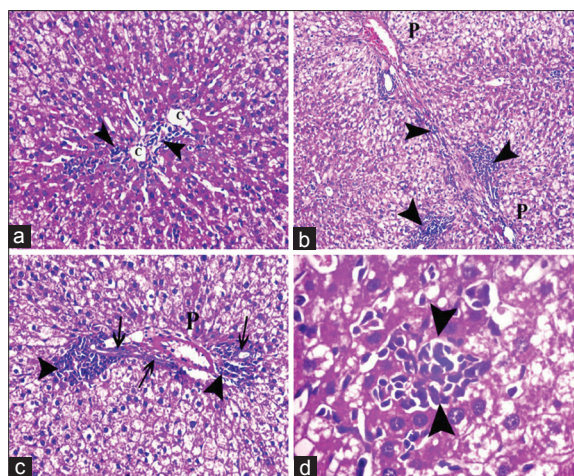


**Figure 4:** Photomicrographs of liver sections of Group III showing cellular infiltrations (arrowhead). (a) Infiltrations around and in between central veins (C). (b and c) Infiltrations around and in between the components of portal tract (P) with proliferation of bile ductules (arrow). (d) Infiltrations between the hepatocytes. Notice most of the hepatocytes are vacuolated (a and c: H and E,  $\times 400$ , b: H and E,  $\times 200$ , d: H and E,  $\times 1000$ )

hepatocytes and blood sinusoids [Figure 9c]. Kupffer cells with indented nuclei and multiple dense bodies were seen lining the blood sinusoids [Figure 9d].

#### Group II (pomegranate-treated group)

Examination of ultrathin sections of livers obtained from animals received pomegranate juice for 6 weeks showed the normal electron microscopic picture of the liver as that of the control group.

#### Group III (fatty liver-induced group)

Examination of ultrathin sections of livers obtained from animals of this group revealed multiple ultrastructural changes in the form of many lipid droplets with variable size and shape within the cytoplasm of the hepatocytes [Figure 10] with dilatation of rER [Figure 10a and b], rarefaction of cytoplasm, and structural changes of mitochondria in the form of enlargement and destruction with complete or partial loss of their cristae [Figure 10c]. Nuclei of most hepatocytes showed, condensed chromatin, irregularity, indentation [Figure 10b], and widening of the perinuclear space [Figure 10a]. Many Ito cells [Figure 10d and e], bundles of collagen fibers [Figure 10e], and inflammatory cells [Figure 10f] were seen between hepatocytes.

#### Group IV (protective group)

Examination of ultrathin sections of livers obtained from animals of both subgroups showed preservation of the normal ultrastructure in most of the animals [Figure 11a and b], except for the presence of many lipid droplets [Figure 11c and d], rarified cytoplasm of [Figure 11d], and condensation of chromatin few hepatocytes [Figure 11f]. Bundles of collagen fibrils were observed in between few hepatocytes [Figure 11f].

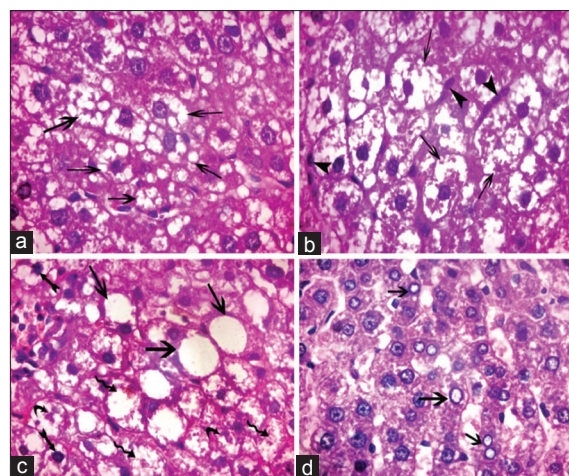


**Figure 5:** Photomicrograph of liver sections of Group III showing hepatocytes with variable cytoplasmic vacuolation. (a) Multiple small vacuoles (arrow) (b) large coalesced vacuoles (arrow) and multiple small cells with ovoid nuclei arranged in rows in between the hepatocytes (arrowheads). (c) Ballooned hepatocytes containing one large vacuole (arrow), some hepatocytes with darkly stained nuclei (biffed arrow), fragmented nuclei (curved arrow), and lysed nuclei (waved arrow). (d) Some hepatocytes with vacuolated nuclei (arrow) (H and E,  $\times 1000$ )

### Morphometric results and statistical analysis

#### I-Area % of collagen fibers

As assessed by image analyzer, pomegranate-received group, revealed a nonsignificant change in the mean area % of collagen fibers as compared to control group. The fatty liver-induced group showed a statistically significant increase in the mean area % as compared to control group. Concerning the protective group, it was found that there was a nonsignificant change in the mean area percentage as compared to control group and showed significant decrease as compared to fatty liver induced group, [Table 1 and Histogram 1].

#### II-Number of glial fibrillary acidic protein +ve cells

As assessed by image analyzer, pomegranate-received group revealed a nonsignificant change in the number of GFAP +ve cells as compared to control group. The fatty liver-induced group showed a statistically significant increase in the number of GFAP +ve cells as compared to control group. There were nonsignificant change in the number of GFAP +ve cells of both protective groups (subgroup IVa and subgroup IVb) as compared to control group, while these groups showed a significant decrease as compared to fatty liver-induced group, [Table 2 and Histogram 2].

#### III-Lipid profile

Results of biochemical analysis showed that pomegranate-received group revealed a nonsignificant change in the levels of TC, TGs, and HDL-c as compared to the control group. The fatty liver-induced group (Group III) showed a statistically significant increase in the levels of TC and TGs and a significant decrease in the level of HDL-c as compared to control group. Concerning the protective group, it was found that there was nonsignificant change in the levels



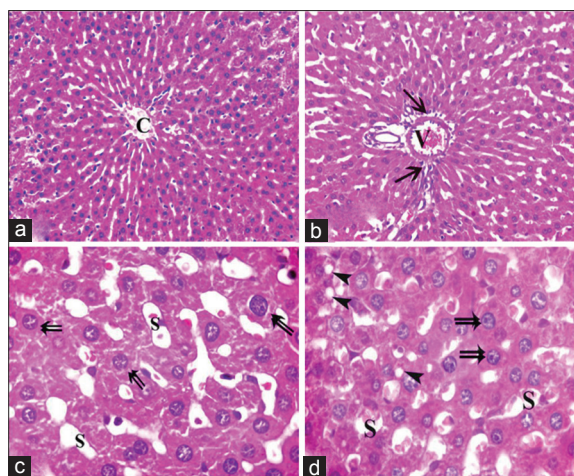


**Figure 6:** Photomicrographs of liver sections of Group IV showing apparently mild dilatation and congestion of central vein (C), portal vein (V) blood sinusoids (S) with mild cellular infiltrations (arrow) around components of a portal tract. Most of hepatocytes appear normal (double arrow) and few cells containing some cytoplasmic vacuoles (arrowhead) (H and E, [a and b]  $\times 400$  [c and d]  $\times 1000$ )

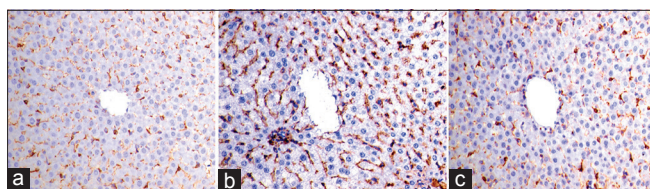


**Figure 8:** Photomicrographs of glial fibrillary acidic protein immunohistochemical-stained liver sections showing (a) glial fibrillary acidic protein-positive cells inbetween the hepatocytes. (b) Apparent increase in number of glial fibrillary acidic protein-positive cells in sections obtained from fatty liver-induced group. (c) Protective group showing apparent decrease in number of glial fibrillary acidic protein-positive cells (glial fibrillary acidic protein immune-reaction,  $\times 400$ )

of TC, TGs and HDL-c as compared to the control group and showed significant decrease in the levels of TC and TGs and a significant increase in the level of HDL-c as compared to fatty liver-induced group, [Tables 3-5 and Histograms 3-5].

## DISCUSSION

NAFLD is a major health problem and considered as the most common worldwide liver disease. Pomegranate is one of the oldest edible fruits and is extensively cultivated in the Mediterranean area. It has antimicrobial, antiparasitic, antiviral, and anticancer effects. It was proved that it lowers blood sugar,<sup>[15]</sup> inhibits low-density lipoprotein oxidation,<sup>[16]</sup> and atheromatous plaque formation.<sup>[17]</sup> The present study aimed to investigate the protective role of pomegranate against experimentally induced fatty liver in adult male albino rats.

The pathogenesis of NAFLD and nonalcoholic steatohepatitis (NASH) is not fully understood. It was explained as prolonged overnutrition that leads to accumulation of free fatty acids and TGs within the liver (steatosis) and progression of NAFLD to NASH that is associated with other

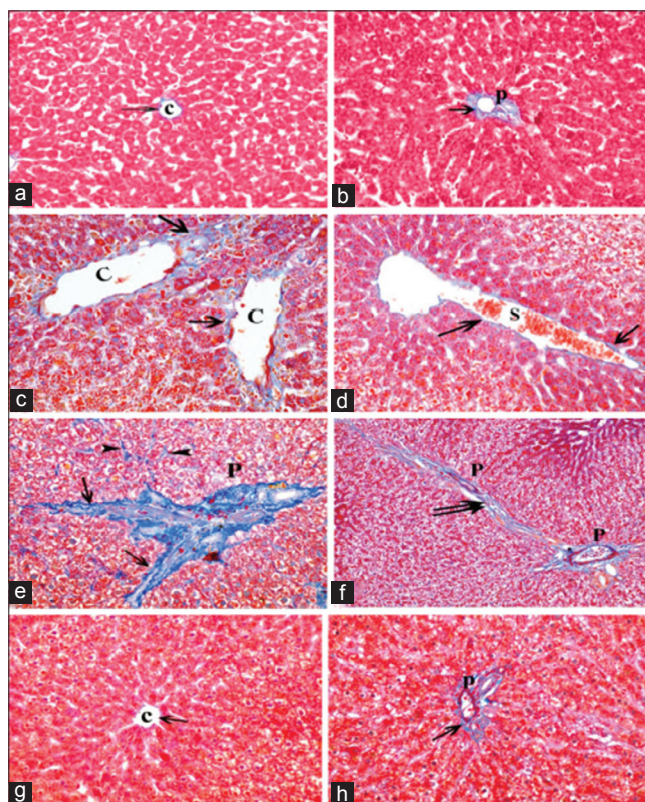


**Figure 7:** Photomicrographs of liver sections showing collagen fibers (arrow) around the central vein (C) and the components of a portal tract (P). (a and b) showing fine collagen in control group. (c-f) Apparent increase in the amount of collagen fibers around dilated central veins, components of a portal tract, dilated congested blood sinusoids (S), and extending in-between the lobules (double arrow) as well as between the cords of hepatocytes (arrowhead). (g and h) Showing fine collagen fibers (arrow) around the central vein and portal tract in protective group (Mallory's trichrome a-h:  $\times 400$ , f:  $\times 200$ )

factors such as oxidant stress, mitochondrial injury, fatty acids lipotoxicity, innate immunity, and inflammatory cytokines. Steatosis is a characteristic histological feature of NAFLD results from increased fatty acid influx or impaired fatty acid utilization in the hepatocytes.<sup>[18]</sup>

Livers obtained from fatty liver-induced group in this research showed yellowish, enlarged livers that were extensively infiltrated with yellow spots on macroscopic examination. These yellow spots may be due to deposition of fat inside hepatic cells, this can be attributed to sinusoidal dilatation, microvesicular steatosis, or fibrosis resulting from an increase in connective tissue following hepatocellular necrosis.<sup>[19]</sup>

Disturbed hepatic architecture of the liver which observed in this study was explained as a result of oxidative damage in hepatocellular proteins or necrotic changes in hepatocytes that lead to irregularity in the orientation of the hepatocyte plates and disturbing hepatic architecture.<sup>[20]</sup> Dilatation of central veins, blood sinusoids, and portal veins were attributed to inflammatory changes or ischemia and hypoxia following high-fat diet.<sup>[21]</sup> The dilatation also might be due to developing hypertension after obesity induced by high-fat diet.<sup>[22]</sup>



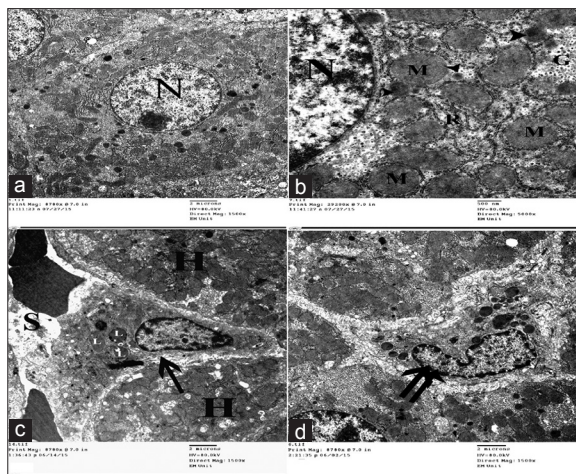


**Figure 9:** Electron micrographs of liver ultrathin sections of control group showing (a) Polyhedral-shaped hepatocyte-containing large rounded nucleus (N) with extended chromatin and prominent nucleolus. (b) The cytoplasm-containing abundant mitochondria (M), rER (R), glycogen granules (G), and multiple peroxisomes (arrowhead). (c) Space of Disse between hepatocytes (H) and blood sinusoids (S) containing HSCs cell (arrow) with multiple lipid with droplets (L). (d) Kupffer cell (double arrow) appears as irregular shaped cell with indented nucleus and multiple cytoplasmic dense bodies

Cellular infiltrations around and between central veins, portal tracts, and even between hepatocytes confirm data obtained by the previous study.<sup>[23]</sup> Moreover, the presence of lobular or acinar infiltration with lymphocytes and neutrophils was observed by other investigators,<sup>[24]</sup> they considered this results as one of the diagnostic features of steatohepatitis. It was reported that the adipocytes in fatty liver are considered as active cells that secrete multiple immune modulator factors in the form of pro-inflammatory cytokines, interleukin-6 and tumor necrotic factor- $\alpha$  with reactive oxygen species (ROS), all these factors contribute to the chronic inflammatory condition and the hepatocytes injury. In addition, inflammatory infiltration can be explained as in severe fatty liver disease; simple steatosis may progress to fibrosing steatohepatitis with initiation of capillarization of the sinusoids. The latter is characterized structurally by a progressive loss of fenestrae in the sinusoidal endothelial cells, concomitant with development of a basal lamina, and deposition of collagen in the space of Disse. This may be accompanying adhesion of leukocytes to the sinusoidal endothelium, followed by leukocyte infiltration into the hepatic parenchyma to form inflammatory foci.<sup>[25]</sup>

Ductular proliferation at the portal tract has been correlated with insulin resistance, impaired hepatocellular replication, and advanced stages of fibrosis, indicating progressive fibrosis.<sup>[26]</sup> It was proved recently the evidence of epithelial-to-mesenchymal transition of ductular epithelial cells through activation of the hedgehog pathway in which mature epithelial cells differentiate into cells with a mesenchymal phenotype and function in NAFLD.<sup>[27]</sup>

Vacuolation of hepatocytes was described as microvesicular and macrovesicular steatosis.<sup>[28]</sup> Macrovesicular steatosis

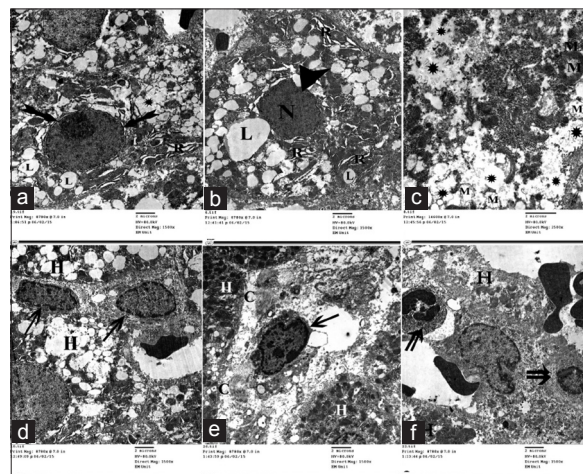


**Figure 10:** Electron micrographs of liver ultrathin section of Group III showing many lipid droplets with variable size and shape (L) within the cytoplasm of the hepatocytes. (a and b) dilatation of rER (R). (c) Rarefaction of cytoplasm (\*) and degenerative changes of mitochondria (M). (a and b) Nuclei of many hepatocytes showing condensed chromatin (N), irregularity, indentation (arrowhead) with widening of the perinuclear space (biffed arrow). (d and e) Many HSCs (arrow), bundles of collagen fibers (C). (f) Inflammatory cells (double arrow) present between the hepatocytes

is explained as abnormalities in the delivery, metabolism, synthesis, and export of lipids. However, microvesicular steatosis which is the hallmark of liver diseases is associated with defective beta-oxidation of fatty acids including mitochondrial cytopathies.<sup>[29]</sup> Furthermore, cytoplasmic vacuolation was attributed to lipid peroxidation because of oxidative stress that damage cell membrane as well as membranes of cell organelles leading to increase in their permeability and disturbance of the ions concentrations in the cytoplasm and cell organelles.<sup>[30,31]</sup> Ballooned hepatocytes can be attributed to microtubular disruption and severe cell injury.<sup>[29]</sup> While rarefaction of the cytoplasm may be due to proliferation of smooth endoplasmic reticulum and glycogen accumulation.<sup>[32]</sup> Mitochondrial abnormalities that were observed in the present study coincided with the previous results and attributed to decreased intramitochondrial protein synthesis, respiratory chain dysfunction, and increase of cytosolic calcium caused by oxidative stress.<sup>[32]</sup> Enlarged mitochondria was represented as an adaptive process to oxidative stress<sup>[33]</sup> or suppression of mitochondrial division because of lowered protein synthesis,<sup>[34]</sup> while dilated rER may be due to lipid peroxidation.<sup>[35]</sup>

The hepatocellular injury was explained by two major mechanisms.<sup>[36]</sup> The direct one involves direct cytotoxicity of the fatty acids on the hepatocytes as a result of excessive intracellular fatty acid accumulation, while the indirect mechanism involves cytotoxic effects of lipid peroxidation of fatty acids. Furthermore, oxidative stress is thought to be the main mechanism of hepatocellular injury as proved by many experimental studies.<sup>[37]</sup> Sources of oxidative stress in NASH include cytochrome P450, peroxisomal-oxidation, mitochondrial dysfunction, and inflammatory cytokines.<sup>[38]</sup>

The nuclear changes were attributed to mitochondrial dysfunction with subsequent decrease in oxidative phosphorylation that leads to decrease in cellular ATP. With prolonged depletion of ATP, structural disruption of protein synthetic apparatus occurs, and irreversible damage to mitochondrial and lysosomal membranes followed by cell necrosis.<sup>[39]</sup> Nuclear vacuolation of some hepatocytes was also detected and was named by pathologists as glycogenated

nuclei which may be due to accumulation of glycogen in the nuclei, and this is a common finding in liver biopsies with Wilson disease, diabetes, and NAFLD.<sup>[28]</sup>

Previous studies<sup>[40]</sup> reported that high-fat diet increased serum hepatic enzyme levels, alanine aminotransferase (ALT) and aspartate aminotransferase (AST). This increase was due to an increase in the production of free radicals that initiate lipid peroxidation. Cellular damage resulted from induction of cytochrome P-450 in the liver producing highly reactive trichloromethyl free radical. This in turn in the presence of oxygen generated by metabolic leakage from mitochondria causes lipid peroxidation of membrane leading to loss of integrity of cell membranes and damage of hepatic cells.

The present work showed significant increase in the collagen fibers deposition and numbers of hepatic stellate cells as was detected in Mallory's trichrome-stained sections and GFAP-stained sections, respectively. This was confirmed by electron microscopic examination in the form of presence of many HSCs and presence of bundles of collagen fibers between hepatocytes. These findings may be attributed to activation of HSCs that leads to fibrosis. There is a cross-link between liver sinusoidal endothelial cells (LSECs) and hepatic stellate cells, healthy LSECs prevent activation of hepatic stellate cells, and inactivate the activated ones. Before hepatic fibrosis LSECs develop an altered phenotype called capillarization that lose the ability to prevent hepatic stellate cell activation and inactivate activated hepatic stellate cells.<sup>[41]</sup> Moreover, in fatty liver, the transforming growth factor-beta (TGF-β) is elevated and

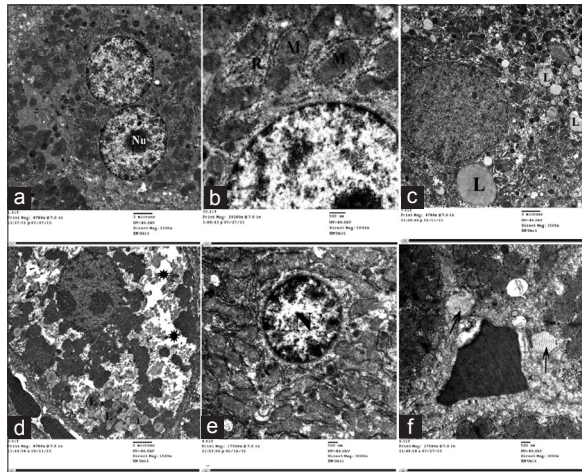
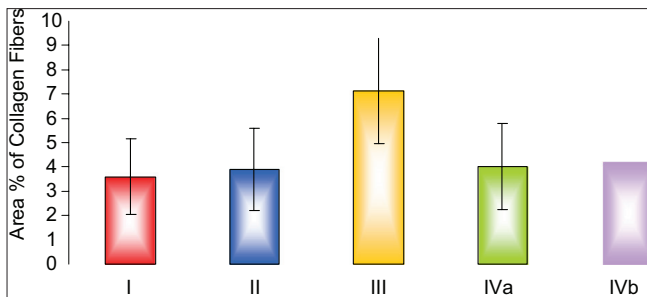
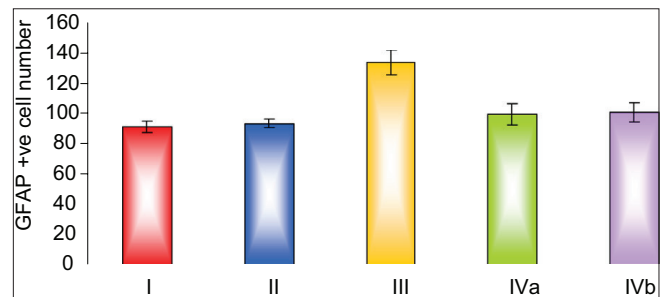


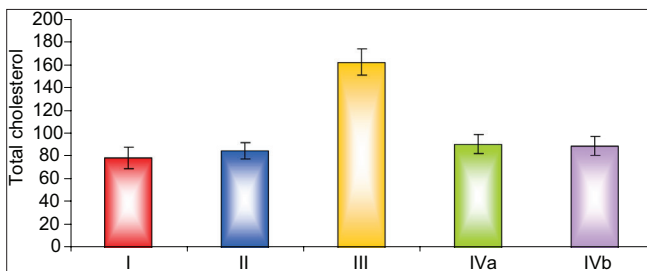
**Figure 11:** Electron micrographs of liver ultrathin section of Group IV showing (a) Multiple hepatocytes some of them are binucleated with prominent nucleolus (Nu), (b) Preserved ultrastructural picture including mitochondria (M) and rough endoplasmic reticulum (R). (c) Others showing many lipid droplets (L). (d) Rarefied cytoplasm (\*). (e) Nuclei with condensed chromatin (N) and (f) Bundles of collagen fibers (arrow) in between the hepatocytes



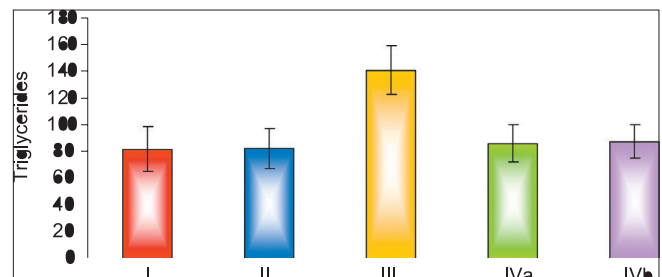
**Histogram 1:** Comparison between the different groups as regard mean ± standard deviation of the area % of collagen fibers. \* $P \leq 0.05$  was considered statistically significant



**Histogram 2:** Comparison between the different groups as regard mean ± standard deviation of the number of glial fibrillary acidic protein +ve cells



**Histogram 3:** Comparison between the different groups as regard mean ± Standard deviation of the total cholesterol level



**Histogram 4:** Comparison between the different groups as regard mean ± Standard deviation of the triglycerides level



**Table 1: Comparison between the different groups as regard mean±SD of the area % of collagen fibers.**

Area % of Collagen Fibers	Control I	Pomegranate II	Fatty liver induced group III	Protective IVa	Protective IVb
Mean±SD	3.59±1.56	3.89±1.69	7.13±2.15	4.03±1.77	4.21±1.80
F value	3.868				
P value	0.014*				
I & II	I & III	I & IVa	I & IVb	III & IVa	III & IVb
0.781	0.002*	0.677	0.558	0.006*	0.010*

**Table 2: Comparison between the different groups as regard mean±SD of the number of GFAP+ve cells. \*P≤0.05 was considered significant.**

GFAP+ve cell number	Control I	Pomegranate II	Fatty liver induced group III	Protective IVa	Protective IVb
Mean±SD	90.83±3.92	92.83±2.86	132.67±8.12	98.83±7.17	100.33±6.38
F value	47.783				
P value	0.001*				
I & II	I & III	I & IVa	I & IVb	III & IVa	III & IVb
0.570	0.001*	0.074	0.062	0.001*	0.001*

**Table 3: Comparison between the different groups as regard mean±SD of the total cholesterol level. \*P≤0.05 was considered significant.**

Total cholesterol	Control I	Pomegranate II	Fatty liver induced group III	Protective IVa	Protective IVb
Mean±SD	78.86±9.19	85.0±7.44	162.43±11.31	90.86±8.09	89.29±8.04
F value	104.687				
P value	0.001*				
I & II	I & III	I & IVa	I & IVb	III & IVa	III & IVb
0.207	0.001*	0.077	0.082	0.001*	0.001*

**Table 4: Comparison between groups as regard mean±SD of the triglycerides level. \*P≤0.05 was considered significant**

Triglycerides	Control I	Pomegranate II	Fatty liver induced group III	Protective IVa	Protective IVb
Mean±SD	81.71±16.85	82.0±14.83	140.43±18.03	86.0±13.81	87.29±12.31
F value	19.042				
P value	0.001*				
I & II	I & III	I & IVa	I & IVb	III & IVa	III & IVb
0.972	0.001*	0.604	0.501	0.001*	0.001*

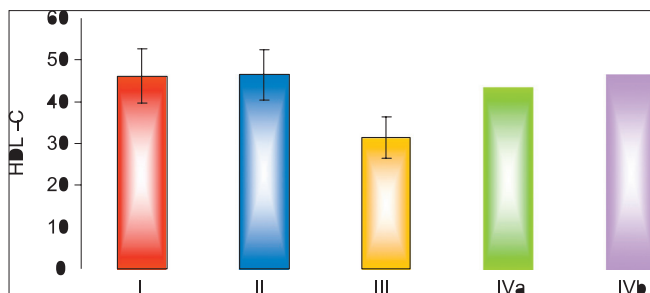
**Table 5: Comparison between the different groups as regard mean±SD of the HDL-c level. \*P≤0.05 was considered significant.**

HDL – c	Control I	Pomegranate II	Fatty liver induced group III	Protective IVa	Protective IVb
Mean±SD	46.14±6.47	46.43±6.08	31.43±4.99	43.57±5.99	46.43±5.29
F value	8.739				
P value	0.001*				
I & II	I & III	I & IVa	I & IVb	III & IVa	III & IVb
0.927	0.001*	0.413	0.927	0.001*	0.001*

correlated closely with collagen gene transcription and scar formation. HSCs are the major targets for TGF- $\beta$  that exerts effects on them leading to their activation with concomitant extracellular matrix production.<sup>[42]</sup>

Results of the present study revealed that feeding of rats on high-fat diet resulted in significant increase in serum levels of TC and TGs accompanied with a significant decrease in HDL-c

level as compared to the control group. These results could be explained on the basis that feeding of rats with high-fat diet leads to an increase in cholesterol absorption and hence an increase in serum cholesterol and TGs.<sup>[43]</sup> Hyperlipidemia may be also due to a decrease in catecholamine level which leads to low  $\beta$ 2-adrenergic receptor function and decrease lipolysis that help in decreasing fat catabolism and increasing the circulating



**Histogram 5:** Comparison between the different groups as regard mean  $\pm$  standard deviation of the high-density lipoprotein cholesterol level

lipid levels.<sup>[44]</sup> The reduction in HDL cholesterol level in animals fed high-fat diet in the present study may be due to the decrease in the enzyme involved in the transesterification of cholesterol, the maturation of HDL, and the flux of cholesterol from cell membranes into HDL.<sup>[45]</sup>

Hepatic stellate cells (HSCs) also known as perisinusoidal cells, lipocytes, fat-storing cells, or Ito cells. They are identifiable by prominent intracellular lipid droplets and by cytoplasmic filamentous material which form the basis for GFAP detection by immunohistochemistry. In comparison with the control group, fatty liver-induced group showed strong positive immune expression of HSC markers "GFAP." This result could be explained by the findings of some researchers<sup>[32]</sup> who stated that GFAP expression in the liver is linked to liver fibrosis and inflammatory infiltration, as activated HSCs secreted cytokines that attracted inflammatory cells. Further, many researchers had been reported the activation of HSC may be closely related to the role of ROS and oxidative stress in stimulating the expression of proinflammatory and profibrotic molecules.<sup>[46]</sup>

In the present work, it was observed that daily administration of pomegranate juice either with or before high-fat diet ameliorate the previous changes. These results agree with findings of other researchers.<sup>[47]</sup> In this regard, it was reported that pomegranate juice had a protective effect against carbon tetrachloride-induced hepatic damage in rats,<sup>[48]</sup> this effect could be attributed to the radical scavenging antioxidant constituents. The principal antioxidant polyphenols in pomegranate juice include the ellagitannins and anthocyanins which have been shown to be the antioxidant responsible for scavenging the free radicals.<sup>[49]</sup> In addition, antioxidant effect of flavonoids that found in pomegranate enhanced the process of regeneration; this might be due to the destruction of free radicals, supplying a competitive substrate for unsaturated lipids in the membrane and/or accelerating the repair mechanism of damaged cell membrane.<sup>[50]</sup>

The antioxidant activity of pomegranate components has been the subject of many studies.<sup>[51]</sup> This activity was shown to be three times higher than that of red wine and green tea, based on the evaluation of the free radicals scavenging activity and iron reducing capacity of the pomegranate juice.<sup>[49]</sup> Pomegranate juice was also shown to have significantly higher levels of antioxidants in comparison to commonly consumed fruit

juices, such as grape, cranberry, grapefruit, or orange juice.<sup>[52]</sup> Furthermore, pomegranate extract has also been shown to preserve the antioxidant enzymes catalase, glutathione peroxidase, and superoxide dismutase from the effects of toxic chemicals<sup>[53,54]</sup> whereas, other study<sup>[55]</sup> reported that pretreatment with pomegranate flower extract for a week had a protective effect against ferric nitrilotriacetate-induced oxidative stress, as well as hepatic injury. This was due to an inhibition of AST and ALT enzymes which may be due to potent antioxidant and hepatoprotective properties of pomegranate. In addition, the ability of pomegranate extract to protect DNA and preventing chromosomal damage in mice was proved.<sup>[56]</sup> Another study revealed that pomegranate flower-activated peroxisome proliferator-activated receptor that decreased cardiac uptake, circulated lipids, cardiac tissue triglyceride content, and plasma TC.<sup>[57]</sup>

In this research, the treatment with pomegranate caused a detectable decrease of the collagen fibers; these effects could be related to its antioxidant, antifibrotic, and antiapoptotic properties.<sup>[58]</sup> Pomegranate juice either with or before high-fat diet can protect against developing changes caused by high-fat diet and reduce risk for development of NAFLD. These findings agree with many studies in recent years that demonstrated a correlation between the role of pomegranate peel extract and juice in regulating vital cellular functions, including cell proliferation and differentiation and its potent antioxidant activity and free radical scavenging capability.<sup>[59]</sup>

## CONCLUSION

The present study concluded that pomegranate juice has a protective role against developing nonalcoholic fatty liver and improving the lipid profile. Therefore, drinking pomegranate juice may be beneficial for persons having risk factors of developing fatty liver or hypercholesterolemia.

## Financial support and sponsorship

Nil.

## Conflicts of interest

There are no conflicts of interest.

## REFERENCES

1. Waugh A, Grant A. Ross and Wilson Anatomy and Physiology in Health and Illness. 9<sup>th</sup> ed. Edinburgh: Elsevier; 2001. p. 307-10.
2. Korish AA, Arafah MM. Camel milk ameliorates steatohepatitis, insulin resistance and lipid peroxidation in experimental non-alcoholic fatty liver disease. *BMC Complement Altern Med* 2013;13:264.
3. Tan Y, Lao W, Xiao L, Wang Z, Xiao W, Kamal MA, *et al.* Managing the combination of nonalcoholic fatty liver disease and metabolic syndrome with Chinese herbal extracts in high-fat-diet fed rats. *Evid Based Complement Alternat Med* 2013;2013:306738.
4. Eshwaraiah MC, Kavitha MN, Bardalai D. Evaluation of hepatoprotective activity of ethanolic root extract of *Punica granatum*. *Int J Pharm Pharm Sci* 2013;5:220-3.
5. Agha FE, Hasannane MM, Omara EA, Hasan AM, El Tomy SA. Protective effect of *Punica granatum* peel extract against pentachlorophenol induced oxidative stress, cytogenetic toxicity and hepatic damage in rats. *Aust J Basic Appl Sci* 2013;7:853-64.



6. Fyiad AA, Abd El-Kader MA, Abd El-Haleem AH. Modulatory effects of pomegranate juice on nucleic acids alterations and oxidative stress in experimentally hepatitis in rats. *Life Sci J* 2012;9:676-82.
7. Yao J, Zhi M, Minhu C. Effect of silybin on high-fat-induced fatty liver in rats. *Braz J Med Biol Res* 2011;44:652-9.
8. Hadipour-Jahromy M, Mozaffari-Kermani R. Chondroprotective effects of pomegranate juice on monoiodoacetate-induced osteoarthritis of the knee joint of mice. *Phytother Res* 2010;24:182-5.
9. Ha AW, Kim WK. The effect of fucoxanthin rich powder on lipid metabolism in rats with a high fat diet. *Nutr Res Pract* 2013;7:287-93.
10. Margoni A, Perrea DN, Vlachos I, Prokopaki G, Pantopoulou A, Fotis L, *et al.* Serum Leptin, adiponectin and tumor necrosis factor- $\alpha$  in hyperlipidemic rats with/without concomitant diabetes mellitus. *Feinstein Inst Med Res* 2011;17:36-40.
11. Kiernan AJ. *Histological and Histochemical Methods: Theory and Practice*. 4<sup>th</sup> ed. Bloxham UK: Scion; 2008. p. 274.
12. Leong AS. *Principles and Practice of Medical Laboratory Science: Basic Histotechnology*. 1<sup>st</sup> ed., Vol. I. Philadelphia: Saunders Company; 1996. p. 171.
13. Baratta JL, Ngo A, Lopez B, Kasabwalla N, Longmuir KJ, Robertson RT, *et al.* Cellular organization of normal mouse liver: A histological, quantitative immunocytochemical, and fine structural analysis. *Histochem Cell Biol* 2009;131:713-26.
14. Woods A, Stirling J. *Electron microscope*. In: Bancroft J, Gamble M. *Theory and Practice of Histological Techniques*. 6<sup>th</sup> ed. Elsevier: Churchill Livingstone Elsevier; 2008. p. 600.
15. Jafri MA, Aslam M, Javed K, Singh S. Effect of *Punica granatum* linn. (flowers) on blood glucose level in normal and Alloxan-induced diabetic rats. *J Ethnopharmacol* 2000;70:309-14.
16. Aviram M, Dornfeld L, Rosenblat M, Volkova N, Kaplan M, Coleman R, *et al.* Pomegranate juice consumption reduces oxidative stress, atherogenic modifications to LDL, and platelet aggregation: Studies in humans and in atherosclerotic apolipoprotein E-deficient mice. *Am J Clin Nutr* 2000;71:1062-76.
17. Fadavi A, Barzegar M, Hossein Azizi M. Determination of fatty acids and total lipid content in oilseed of 25 pomegranates varieties grown in Iran. *J Food Compos Anal* 2006;19:676-80.
18. Mahtab MA, Fazle Akbar SM. Non-alcoholic fatty liver disease: A review. *J Gastroenterol Hepatol Res* 2013;2:439-44.
19. Altunkaynak BZ, Ozbek E. Overweight and structural alterations of the liver in female rats fed a high-fat diet: A stereological and histological study. *Turk J Gastroenterol* 2009;20:93-103.
20. Abraham P, Wilfred G, Ramakrishna B. Oxidative damage to the hepatocellular proteins after chronic ethanol intake in the rat. *Clin Chim Acta* 2002;325:117-25.
21. Arvanitidis AP, Corbett D, Colbourne F. A high fat diet doesn't exacerbate CA1 injury and cognitive deficits following global ischemia in rats. *Brain Res* 2009;1252:192-200.
22. Elahi MM, Cagampang FR, Mukhtar D, Anthony FW, Ohri SK, Hanson MA, *et al.* Long-term maternal high-fat feeding from weaning through pregnancy and lactation predisposes offspring to hypertension, raised plasma lipids and fatty liver in mice. *Br J Nutr* 2009;102:514-9.
23. Tan Y, Lao W, Xiao L, Wang Z, Xiao W, Kamal MA, *et al.* Managing the combination of nonalcoholic fatty liver disease and metabolic syndrome with Chinese herbal extracts in high-fat-diet fed rats. *Evid Based Complement Alternat Med* 2013;2013:306738.
24. Brunt EM, Tiniakos DG. Histopathology of nonalcoholic fatty liver disease. *World J Gastroenterol* 2010;16:5286-96.
25. Schäffler A, Schölmerich J, Büchler C. Mechanisms of disease: Adipocytokines and visceral adipose tissue – Emerging role in nonalcoholic fatty liver disease. *Nat Clin Pract Gastroenterol Hepatol* 2005;2:273-80.
26. Richardson MM, Jonsson JR, Powell EE, Brunt EM, Neuschwander-Tetri BA, Balthal PS, *et al.* Progressive fibrosis in nonalcoholic steatohepatitis: Association with altered regeneration and a ductular reaction. *Gastroenterology* 2007;133:80-90.
27. Syn WK, Jung Y, Omenetti A, Abdelmalek M, Guy CD, Yang L, *et al.* Hedgehog-mediated epithelial-to-mesenchymal transition and fibrogenic repair in nonalcoholic fatty liver disease. *Gastroenterology* 2009;137:1478-88.e8.
28. Brunt EM, Tiniakos DG. Alcoholic and non-alcoholic fatty liver disease. In: Odze RD, Goldblum JR, Crawford JM, editors. *Pathology of the GI Tract, Liver, Biliary Tract and Pancreas*. Philadelphia: Saunders; 2009. p. 1087-114.
29. Tiniakos DG, Kittas CH. Pathology of nonalcoholic fatty liver disease. *Ann Gastroenterol* 2005;18:148-59.
30. Panqueva RP. Pathological aspects of fatty liver disease. *Rev Col Gastroenterol* 2014;29:72-8.
31. Emanuel R. *Essential Pathology*. 3<sup>rd</sup> ed., Ch. 1. Lippincott Williams & Wilkins; 2001. p. 1.
32. Lotowska JM, Sobaniec-Lotowska ME, Bockowska SB, Lebensztejn DM. Pediatric non-alcoholic steatohepatitis: The first report on the ultrastructure of hepatocyte mitochondria. *World J Gastroenterol* 2014;20:4335-40.
33. Le TH, Caldwell SH, Redick JA, Sheppard BL, Davis CA, Arsenau KO, *et al.* The zonal distribution of megamitochondria with crystalline inclusions in nonalcoholic steatohepatitis. *Hepatology* 2004;39:1423-9.
34. Monroe W. Value of electron microscopy analysis for diagnosis of mitochondrial cytopathy. *American Society for Clinical Pathology*; 2004. p. 15.
35. Dai XF, Chen DF. Liver regenerative capacity after partial hepatectomy in rats with nonalcoholic fatty liver disease. *Zhonghua Gan Zang Bing Za Zhi* 2006;14:597-601.
36. Wierzbicki AS, Oben J. Nonalcoholic fatty liver disease and lipids. *Curr Opin Lipidol* 2012;23:345-52.
37. Ma X, Li Z. Pathogenesis of nonalcoholic steatohepatitis (NASH). *Chin J Dig Dis* 2006;7:7-11.
38. Rolo AP, Teodoro JS, Palmeira CM. Role of oxidative stress in the pathogenesis of nonalcoholic steatohepatitis. *Free Radic Biol Med* 2012;52:59-69.
39. Kumar V, Abbas AK, Fausto N. *Cellular adaptation, cell injury and cell death*. Robbins and Cotran Pathologic Basis of Disease. 7<sup>th</sup> ed., Ch. 1. Elsevier: Elsevier Saunders; 2008. p. 3.
40. Saki N, Saki G, Rahim F, Khoozani AS, Nikakhlagh S. Modulating effect of soy protein on serum cardiac enzymes in cholesterol-fed rats. *Int J Med Med Sci* 2011;3:390-5.
41. Xie G, Wang X, Wang L, Wang L, Atkinson RD, Kanel GC, *et al.* Role of differentiation of liver sinusoidal endothelial cells in progression and regression of hepatic fibrosis in rats. *Gastroenterology* 2012;142:918-27.e6.
42. Wiercinska E, Wickert L, Denecke B, Said HM, Hamzavi J, Gressner AM, *et al.* Id1 is a critical mediator in TGF- $\beta$ -induced transdifferentiation of rat hepatic stellate cells. *Hepatology* 2006;43:1032-41.
43. Lim DW, Kim YT, Jang YJ, Kim YE, Han D. Anti-obesity effect of *Artemisia capillaris* extracts in high-fat diet-induced obese rats. *Molecules* 2013;18:9241-52.
44. Al-Awadi JH, Rashid KH, Hassen AJ. High fat diet induce hyperlipidemia incidences with sever changes in liver tissue of male albino rats: A histological and biochemical Study. *Kerbala J Pharm Sci* 2013;6:21-32.
45. Shepherd J. Lipoprotein metabolism. An overview. *Drugs* 1994;47 Suppl 2:1-0.
46. Bayomy NA, Soliman GM, Abdelaziz EZ. Effect of potassium bromate on the liver of adult male albino rat and A possible protective role of Vitamin C: Histological, immunohistochemical, and biochemical study. *Anat Rec (Hoboken)* 2016;299:1256-69.
47. Al-Shaabi SN, Waly MI, Al-Subhi L, Tageldin MH, Al-Balushi NM, Rahman MS, *et al.* Ameliorative effects of pomegranate peel extract against dietary-induced nonalcoholic fatty liver in rats. *Prev Nutr Food Sci* 2016;21:14-23.
48. Rahman Ibrahim MA, Mahmoud Okail HA, Mansour Emam NM. Ameliorative effects of pomegranate peel extract on hepatotoxicity induced by carbon tetrachloride in mice. *Int J Res Stud Biosci* 2016;4:23-31.
49. Gil MI, Tomás-Barberán FA, Hess-Pierce B, Holcroft DM, Kader AA. Antioxidant activity of pomegranate juice and its relationship with phenolic composition and processing. *J Agric Food Chem* 2000;48:4581-9.
50. El-Khadragy MF. Hepatoprotective role of the pomegranate (*Punica granatum*) juice on carbon tetrachloride-induced oxidative stress in rats.

- Afr J Biol Sci 2011;7:135-49.
51. Mousavinejad G, Emam-Djomeh Z, Rezaei K, Khodaparast MH. Identification and quantification of phenolic compounds and their effects on antioxidant activity in pomegranate juices of eight Iranian cultivars. *Food Chem* 2009;115:1274-8.
  52. Rosenblat M, Aviram M. Anti-oxidative properties of pomegranate: *In vitro* studies. In: Seeram NP, Rand Heber DS, editors. *Pomegranates: Ancient Roots to Modern Medicine*. Ch. 2. New York: Taylor and Francis Group; 2006. p. 31.
  53. Chidambara Murthy KN, Jayaprakasha GK, Singh RP. Studies on antioxidant activity of pomegranate (*Punica granatum*) peel extract using *in vivo* models. *J Agric Food Chem* 2002;50:4791-5.
  54. Türk G, Sönmez M, Aydın M, Yüce A, Gür S, Yüksel M, *et al.* Effects of pomegranate juice consumption on sperm quality, spermatogenic cell density, antioxidant activity and testosterone level in male rats. *Clin Nutr* 2008;27:289-96.
  55. Kaur G, Jabbar Z, Athar M, Alam MS. *Punica granatum* (pomegranate) flower extract possesses potent antioxidant activity and abrogates fe-NTA induced hepatotoxicity in mice. *Food Chem Toxicol* 2006;44:984-93.
  56. Valadares MC, Pereira ER, Benfica PL, Paula JR. Assessment of mutagenic and antimutagenic effects of *Punica granatum* in mice. *Braz J Pharm Sci* 2010;46:121-7.
  57. Huang TH, Peng G, Kota BP, Li GQ, Yamahara J, Roufogalis BD, *et al.* Pomegranate flower improves cardiac lipid metabolism in a diabetic rat model: Role of lowering circulating lipids. *Br J Pharmacol* 2005;145:767-74.
  58. Salwe KJ, Sachdev DO, Bahurupi Y, Kumarappan M. Evaluation of antidiabetic, hypolipidemic and antioxidant activity of hydroalcoholic extract of leaves and fruit peel of *Punica granatum* in male wistar albino rats. *J Nat Sci Biol Med* 2015;6:56-62.
  59. Ahmed AT, Belal SK, Elsaid Salem AG. Protective effect of pomegranate peel extract against diabetic induced renal histo-pathological changes in albino rats. *IOSR J Dent Med Sci* 2014;13:94-105.